BMC Biochemistry

BioMed Central

Research article

The Metal Coordination of sCD39 during ATP Hydrolysis

Wei Chen and Guido Guidotti*

Address: Department of Molecular and Cellular Biology, Harvard University, 7 Divinity Avenue, Cambridge, MA 02138, USA

E-mail: Wei Chen - weichen@fas.harvard.edu; Guido Guidotti* - guidotti@fas.harvard.edu

*Corresponding author

Published: 12 September 2001

BMC Biochemistry 2001, **2**:9

Received: 25 July 2001

Accepted: 12 September 2001

This article is available from: http://www.biomedcentral.com/1471-2091/2/9

Abstract

Background: The hydrolysis of ATP and ADP by ecto-nucleoside triphosphate diphosphohydrolase 1 (CD39) requires divalent cations, like Ca^{2+} and Mg^{2+}. In spite of considerable work, it is not clear whether divalent cations bind to the enzyme in the absence of nucleotide or only as nucleotide-Me^{+2} complex. Here we study the protein ligands for Me^{+2}.

Results: When VO^{2+} was used as a substitute for Ca^{2+}, the ATPase activity of soluble CD39 was 25% of that with Ca^{2+} as cofactor. Protein ligands of the VO^{2+}-nucleotide complex bound to the catalytic site of soluble CD39 were characterized by electron paramagnetic resonance (EPR) spectroscopy. The EPR spectrum contained one species designated T with VO^{2+}-AMPPNP as ligand. Two species D1 and D2 were observed when VO^{2+}-AMPCP was bound to soluble CD39. The results suggest that species D1 and D2 represent the metal-ADP complexes at the catalytic site of soluble CD39 corresponding to the intermediate formed during ATP hydrolysis and the substrate for further hydrolysis, respectively.

Conclusions: VO^{2+} can functionally substitute for Ca^{2+} as a cofactor of sCD39, and it produces four different EPR features when bound in the presence of different nucleotides or in the absence of nucleotide. The metal coordination for each conformation corresponding to each EPR species is proposed, and the mechanism of sCD39 catalysis is discussed.

Background

Ecto-Nucleoside triphosphate diphosphohydrolases (E-NTPDases, formerly called ecto-ATPases) hydrolyze nucleotides in the presence of divalent cations and are insensitive to inhibitors of P-type, F-type, and V-type ATPases [1]. Three isoforms that differ in the ratio of ATPase/ADPase activity are present on the cell surface [2]: E-NTPDase1 with a ratio of 1, E-NTPDase2 with a ratio of 10 and E-NTPDase3 with a ratio of 3–5. NTPDases are important in many physiological processes like cell motility, adhesion, nonsynaptic information transfer, secretion, regulation of hemostasis and ectokinases [1]. Understanding the enzymatic mechanisms of the NTPDases will help description of their physiological functions, and development of strategies to regulate the functions of the enzymes.

The catalytic mechanism of NTPDases is not known even though some basic facts of the catalysis have been established. NTPDases do not form phosphorylated intermediates during catalysis, a conclusion also supported by lack of vanadate sensitivity and Pi product inhibition [3–6]. The catalytic reaction appears to be irreversible and no partial reactions have been observed [7,8]. Divalent cations like Ca^{2+} or Mg^{2+} are required for activity, and maximal activity is reached when the concentrations of

substrates and divalent cations are equal [1]. The specific activities of NTPDases vary over a broad range from ten thousand units for potato apyrase to less than one hundred units for chicken gizzard ecto-ATPase [9,10]. Sequence comparisons indicate that most of NTPDases contain five highly conserved regions, apyrase conserved region, ACR1 – ACR5 [9,11]. However, the catalytic sites have not been identified, although ACR1 and ACR4 have been implicated in β- and γ-phosphate binding, respectively [9].

E-NTPDase1 is also called CD39, as it was first described as an antigen present on activated B and T lymphocytes. Residues of ACR1 to ACR5 of CD39 have been mutated to study the involvement of the ACR regions in catalysis. E174 in ACR3 and S218 in ACR4 are required for catalytic function [12]. Substitution of H59 in ACR1 converted CD39 into an ADPase in a quaternary structure dependent manner [13]. Mutation of W187A in ACR3 affected CD39 folding and translocation, while mutation of W459A in ACR5 increased ATPase activity but diminished ADPase activity [14]. Mutations of D62 and G64 of ACR1 and D219 and G221 of ACR4 demonstrated that the nucleotide phosphate binding domains of NTPDases are similar to those present in the actin/heat shock protein/sugar kinase superfamily [15]. These results suggest that the conserved residues of the ACR1 to 5 regions are involved in the catalytic mechanism of CD39.

The catalytic activity of CD39 is dependent on the presence of divalent cations. Since the interactions of Ca^{+2} and Mg^{+2} with proteins are difficult to study due to the lack of spectroscopic properties, vanadyl $(V^{IV}=O)^{2+}$ has been used as a probe of the ligands that compose Mg^{2+}, Ca^{2+}, and Mn^{2+} binding sites of several proteins, including carboxypeptidase [16], S-adenosylmethionine synthetase [17,18], pyruvate kinase [19,20], and F_1-ATPase [21,22]. This cation specifically binds to divalent cation binding sites of several enzymes, and in many cases serves as a functional cofactor [23]. Vanadyl has one axial and four equatorial coordination sites relative to the axis of the double-bounded oxygen, an arrangement that is similar to that for Ca^{2+} and Mg^{2+}. As it is known that the **A** and **g** tensors derived from the EPR spectrum of bound VO^{2+} are a direct measure of the nature of the equatorial metal ligands [24], binding of VO^{2+} to CD39 could provide details about the catalytic mechanism of CD39.

Recently we reported that a recombinant soluble CD39, capable of hydrolyzing both ATP and ADP, was expressed and purified from insect cells [25]. Only one nucleotide-binding site was identified on the purified soluble CD39 in the presence of Ca^{2+} when non-hydrolysable nucleotide analogs were used. In this report, we characterized the signals that were obtained from bound VO^{2+} when ATP or ADP was present at the catalytic site of the purified soluble CD39. The possible metal ligands for VO^{+2} at the catalytic site are proposed and the catalytic mechanism is discussed.

Results

Nucleotidase activity of purified soluble CD39 with VO^{2+} as cofactor

The ability of purified soluble CD39 to hydrolyze VO^{2+}ATP is shown in Figure 1. Soluble CD39 did not hydrolyze either ATP or ADP in the absence of VO^{2+} (Fig. 1A). When VO^{2+} was mixed with ATP at a ratio of 1:1, the concentrations of both ADP and AMP increased and ATP decreased as the incubation time was prolonged (Fig. 1B). The ATPase activity of sCD39 with VO^{2+} was about 25% of that with Ca^{2+} as a cofactor. Vanadyl is unstable in aqueous solution at pH7.0 in the absence of chelator and will precipitate out of solution as $[VO(OH)_2]_n$. The rate of precipitation depends on the abundance and affinity of the chelator. This means that the actual VO^{2+} concentration was lower than 0.5 mM. This result indicates that VO^{2+} can functionally substitute for Ca^{2+} as cofactor for sCD39 nucleotidase activity.

Characterization of bound VO^{2+} ADPNP by CW-EPR

The parallel features of CW-EPR spectrum of bound VO^{2+} in the presence of ADPNP, an ATP analog, are shown in Figure 2a. This spectrum shows ^{51}V hyperfine splitting and the center of the parallel transitions from molecules with the V=O bond oriented along the magnetic field ($A_{||}$, $g_{||}$) which are strong enough to tell the nature of VO^{2+} equatorial ligands [22]. Of the eight transitions that result from the parallel oriented molecules, the $-7/2_{||}$, $-5/2_{||}$, $+3/2_{||}$, $+5/2_{||}$, and $+7/2_{||}$ transitions (shown in the figures from left to right, respectively) do not overlap with perpendicular transitions. The ^{51}V hyperfine splitting spectra from molecules with V=O bond perpendicular to the magnetic field ($A\perp$) are much smaller and not shown here [21]. The intensity of $-5/2_{||}$ peak is used as direct measurement of the amount of bound VO^{2+}, since this peak is the most intense peak in the EPR spectrum that contains contribution only from $A_{||}$ but not $A\perp$ [21,26]. In this study, the intensities of each bound VO^{2+}-EPR feature were normalized to 1 mg of protein.

VO^{2+} bound as the VO^{2+}-AMPPNP complex to sCD39 produced a strong spectrum characterized by $A_{||}$ of 504.25 MHz and $g_{||}$ of 1.9410 (Fig. 2b), called species T (Table 1). The best fit of EPR species T to eq 1 is one equatorial nitrogen from an amino group and three equatorial oxygen ligands from carboxyl or phosphate groups (Table 2). This result is consistent with AMPPNP binding

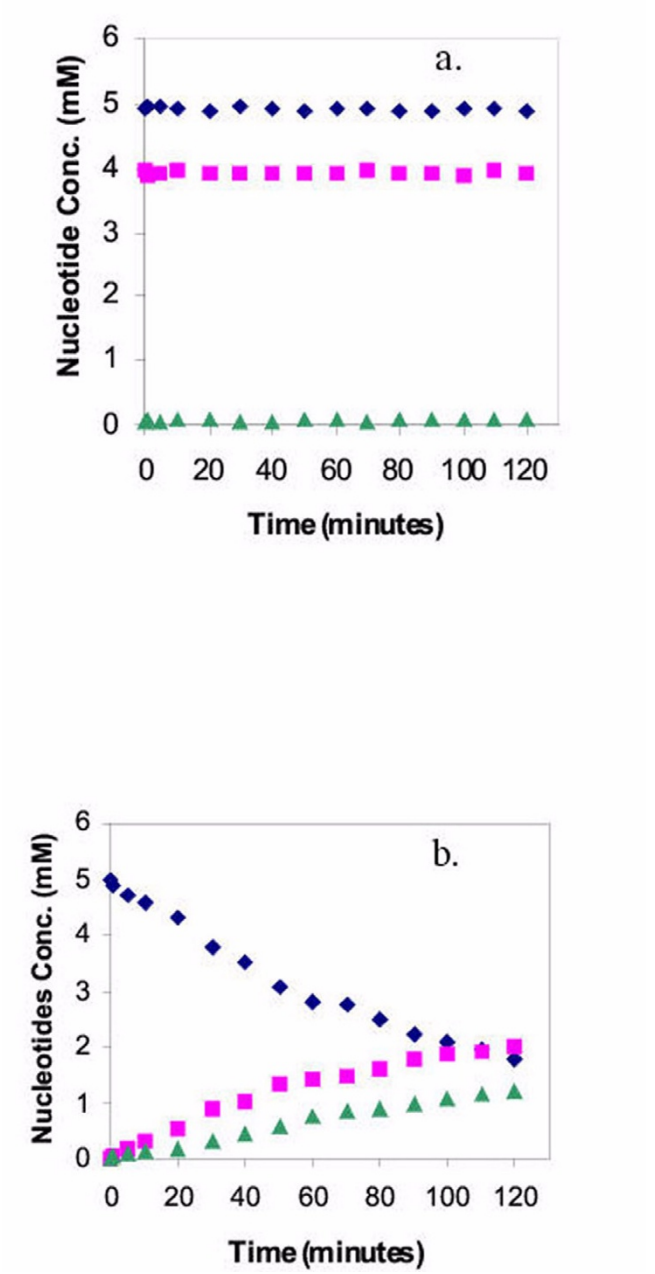

Figure 1
ATP hydrolysis by sCD39 with VO^{2+} as cofactor analyzed by HPLC. 2 μg of sCD39 was included in each assay. A. The reaction was conducted in the presence of 0.5 mM ATP but without VO^{2+}. B. The reaction was initiated by adding 0.5 mM VO^{2+}-ATP (1:1). ATP is represented as black diamonds; ADP as a black square; and AMP as a black triangles;

strongly to a single site on sCD39 in the presence of metal [25].

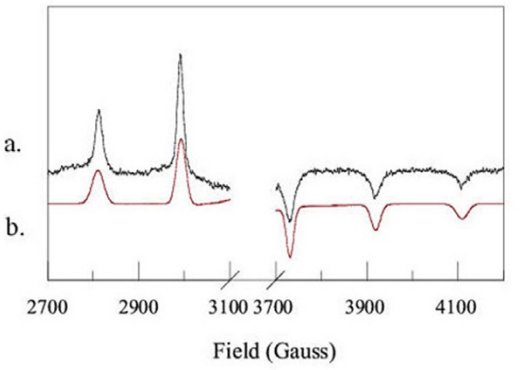

Figure 2
Parallel regions of VO^{2+}-EPR spectrum of VO^{2+}-ADPNP bound to sCD39. a. One mole equivalent of VO^{2+}-ADPNP was added to 2.8 mg of sCD39 as described in Experimental Procedures. EPR conditions were as follows: field modulation frequency, 100 kHz; modulation amplitude, 0.97 G; receive gain, 2×10^4; sweep time 5.243 s; time constant 1.28 ms; micropower, 1.0 mW; microwave frequency 9.40386 GHz, 1000 scans; temperature; 125 K. b. Simulated spectrum was generated by the program QPOWA with the experimental conditions above and $A_{||}$ = 504.25 MHz, $g_{||}$ = 1.9410 for Species T.

Characterization of EPR species from VO^{2+}-AMPCP bound to sCD39

Figure 3a shows the parallel features of the EPR spectrum of sCD39 bound VO^{2+}-AMPCP. Two sets of parallel transitions were observed, and the derived $A_{||}$ and $g_{||}$ values are listed in Table 1. One set had $A_{||}$ of 521.78 MHz and $g_{||}$ of 1.937, which is defined as species D1 (Fig. 3b). The other set displayed $A_{||}$ of 490.01 MHz and $g_{||}$ of 1.9435, which is called species D2 (Fig. 3c). The intensity of species D1 accounted for 11.4% of species T from bound VO^{2+}-AMPPNP, and the intensity of D2 accounted for 7.1% of species T. The intensity ratio of species D1 over D2 was 1.6.

In order to distinguish species D1 from D2, the sample with VO^{2+}-AMPCP bound to sCD39 was thawed and incubated at room temperature for 30 minutes, and the VO^{2+} EPR spectrum was collected again. As shown in Figure 4a and 4b, either $A_{||}$ or $g_{||}$ values for both species D1 and D2 were changed. The intensity of species D1 was not changed as it accounted for 12.1% of the intensity of species T of the bound VO^{2+}-AMPPNP. However, the intensity of species D2 was decreased dramatically, and it accounted for only 0.1% of the intensity of species T. The intensity ratio of D1 over D2 increased about 75 fold to become 120.

Table 1: Experimental signal intensity and ^{51} V-hyperfine parameters derived from the VO^{2+} bound to sCD39 under different conditions.

Nucleotide	Species	Intensity	Experimental Parameters	
		(% of VOADPNP)	$g_{\|\|}$	$A_{\|\|}$
VOADPNP	T	100	1.9410	504.25
VO^{2+}	V	20.3	1.9460	486.00
	D1	11.4	1.9370	521.78
VOAMPCP				
	D2	7.1	1.9435	490.01
VOAMPCP*	D1	12.1	1.9350	521.78
VOATP	D2	7.5	1.9455	489.5
VOATP*	D2	0.2	1.9455	489.5

* Samples were incubated at room temperature for 30 minutes.

Table 2: Best fits of the ^{51} V-hyperfine parameters (Eq. 1) of VO^{2+} bound to various equatorial ligands of sCD39 under different conditions.

Species	Calculated		Most Probable Equatorial Ligands			
	$g_{\|\|}$	$A_{\|\|}$				
T	1.9445	504.25	RNH_2	RCOO	Pi	Pi
D1	1.9390	520.95	H_2O	RCOO	Pi	Pi
D2	1.9435	490.01	ROH	RCOO	RCOO	Pi
V	1.9500	485.36	ROH	ROH	H_2O	H_2O

There are two sets of equatorial ligands that can fit well the EPR species D1 according to Eq 1 (Table 2). One set includes two equatorial oxygen from two water molecules, one equatorial oxygen from a carboxyl group or phosphate, and one equatorial nitrogen from an amino group. The other set contains one equatorial oxygen from water and three equatorial oxygens from carboxyl groups or phosphate. The best fit for the EPR species D2 to eq 1 is one equatorial oxygen from a hydroxyl group and three equatorial oxygens from carboxyl groups or phosphate.

EPR characteristics of sCD39 bound VO^{2+}-ATP

In order to capture the bound VO^{2+}-EPR signal before the enzyme completely turned over, sCD39 and VO^{2+}-ATP were mixed on ice, immediately transferred into the EPR tube and frozen. The entire process took about 15 seconds. The parallel portion of the collected VO^{2+}-EPR spectrum is shown in Figure 5a. VO^{2+}-ATP complex bound to sCD39 produced an EPR spectrum with $A_{||}$ of 489.5 MHz and $g_{||}$ of 1.9455, which corresponded to species D2 (Fig. 5b). The signal intensity from the bound VO^{2+}-nucleotide complex accounted only for 7.5% of that of species T from bound non-hydrolysable VO^{2+}-ADPNP complex.

The same sample made from mixing VO^{2+}-ATP and sCD39 was incubated at room temperature for 30 minutes, then the VO^{2+}-EPR spectrum was generated as shown in Figures 4c and 4d. The EPR parameters derived from this VO^{2+}-EPR spectrum were 489.5 MHz for $A_{||}$ and 1.9455 for $g_{||}$ respectively, which is consistent with species D2. However, the signal intensity decreased about 37.5 fold compared to that obtained before room temperature incubation.

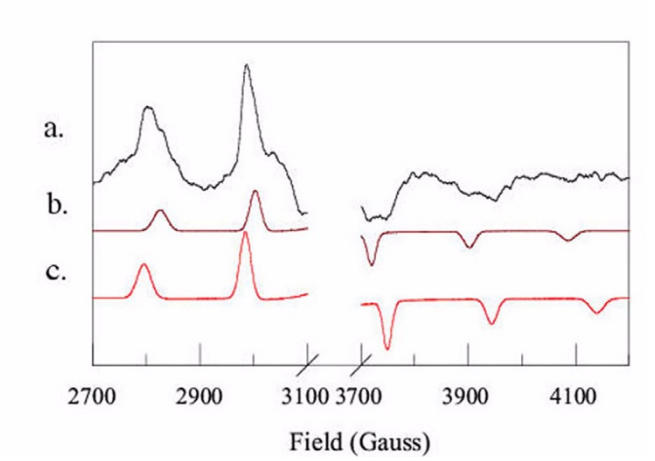

Figure 3
Parallel regions of VO^{2+}-EPR spectrum of VO^{2+}-AMPCP bound to sCD39. a. One mole equivalent of VO^{2+}-AMPCP was added to 6.5 mg of sCD39 prepared as in Experimental Procedures. EPR conditions were as follows: field modulation frequency, 100 kHz; modulation amplitude, 0.97 G; receive gain, 2×10^4; sweep time 5.243 s; time constant 1.28 ms; micropower, 1.0 mW; microwave frequency 9.40677 GHz, 1600 scans; temperature; 125 K. b. Simulated spectrum was generated by the program QPOWA with the experimental conditions above and $A_{||}$ = 521.78 MHz, $g_{||}$ = 1.9370 for Species D1. c. Simulated spectrum was generated by the program QPOWA with the experimental conditions above and $A_{||}$ = 490.01 MHz, $g_{||}$ = 1.9435 for Species D2.

Free VO^{2+} binding to sCD39 characterized by CD-EPR

Like other metals (Ca^{2+} and Mg^{2+}), free VO^{2+} inhibited the nucleotidase activities of sCD39 at high concentration (data not shown). VO^{2+} in the absence of any nucleotides was added to sCD39 at 1:1 molar ratio. The parallel transitions of bound VO^{2+}-EPR spectrum are shown in Figure 6. The features derived from the VO^{2+}-EPR spectrum were 486 MHz for $A_{||}$ and 1.946 for $g_{||}$, which was designed as species V (Fig. 6b). The signal intensity of bound VO^{2+} accounted for 20.3% of that from the bound VO^{2+}-ADPNP complex.

The best fit of equatorial ligands for species V according to eq 1 is two equatorial oxygen from hydroxyl groups and another two equatorial oxygen from two water molecules.

Discussion

Vanadyl has been used to estimate the types of groups that serve as metal-ligands in F_1-ATPase and other enzymes [16,18,19,21] because the g and A tensors of the ^{51}V hyperfine couplings are approximately a linear combination of tensors from each type of group that contributes an equatorial ligand [24,27]. By studying the EPR spectra of bound VO^{2+} in the presence of different nucleotides, we show that the interaction of soluble CD39 with ATP is different from that with ADP.

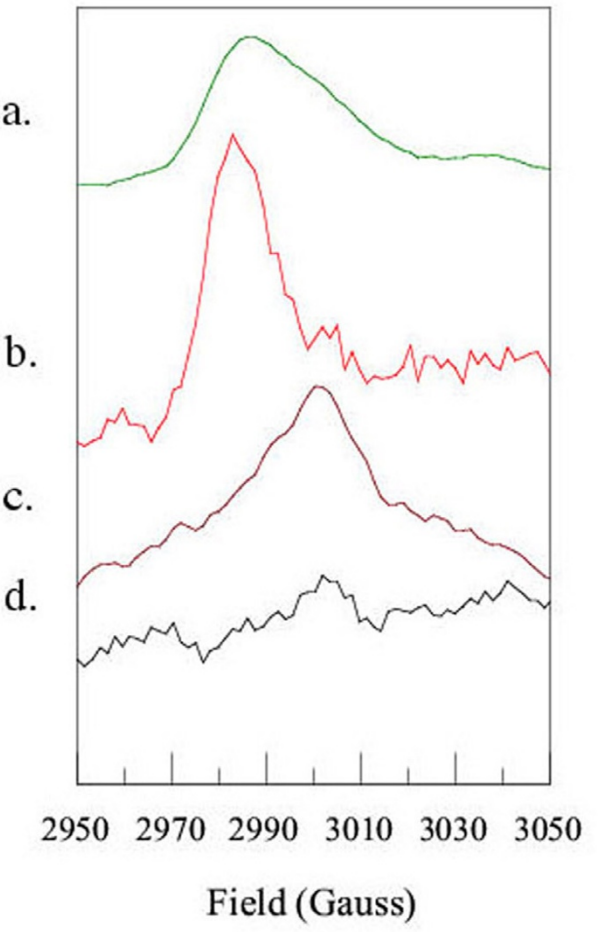

Figure 4
Parallel -5/$2_{||}$ region of VO^{2+}-EPR spectra in the presence of different nucleotides and conditions. a. One equivalent of a 1 : 1 mole ratio of VO^{2+}-AMPPCP was added to sCD39, and incubated on ice for 5 minutes. b. The sample from a was thawed and incubated at room temperature for 30 minutes before collecting data again. c. One equivalent of a 1 : 1 mole ratio of VO^{2+}-ATP was added to sCD39, and frozen immediately in liquid nitrogen. d. The sample from c was thawed and incubated at room temperature for 30 minutes before collecting data again.

It is not surprising that VO^{2+} can functionally replace Ca^{2+} in the hydrolysis of both ATP and ADP by soluble CD39, although the enzymatic activity is about 25% of that with Ca^{2+} as the cofactor, since F_1-ATPase also hydrolyzes ATP at a decreased rate when VO^{2+} replaces Mg^{2+}[21].

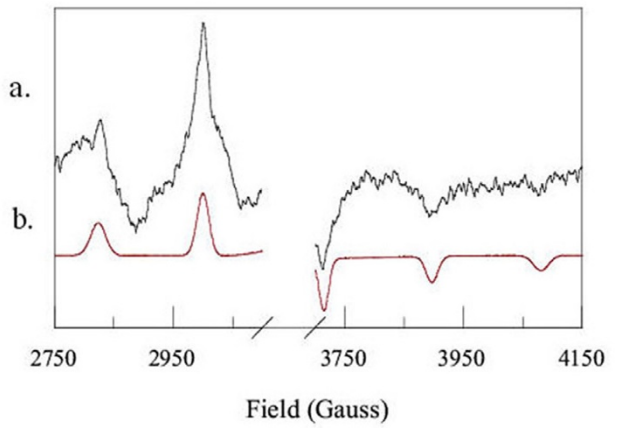

Figure 5
Parallel regions of VO^{2+}-EPR spectrum of VO^{2+}-ATP bound to sCD39. a. One mole equivalent of VO^{2+}-ATP was added to 5.7 mg of sCD39 prepared as in Experimental Procedures. EPR conditions were as follows: field modulation frequency, 100 kHz; modulation amplitude, 0.97 G; receive gain, 2×10^4; sweep time 5.243 s; time constant 1.28 ms; micropower, 1.0 mW; microwave frequency 9.40658 GHz, 3000 scans; temperature; 125 K. b. Simulated spectrum was generated by the program QPOWA with the experimental conditions above and $A_{||}$ = 489.5 MHz, $g_{||}$ = 1.9455 for Species D2.

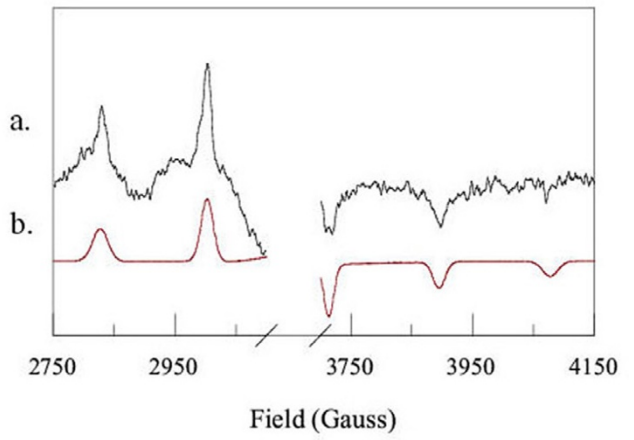

Figure 6
Parallel regions of VO^{2+}-EPR spectrum of free VO^{2+} bound to sCD39. a. One mole equivalent of free VO^{2+} was added to 2.6 mg of sCD39 prepared as in Experimental Procedures. EPR conditions were as follows: field modulation frequency, 100 kHz; modulation amplitude, 0.97 G; receive gain, 2×10^4; sweep time 5.243 s; time constant 1.28 ms; micropower, 1.0 mW; microwave frequency 9.40798 GHz, 3000 scans; temperature; 125 K. b. Simulated spectrum was generated by the program QPOWA with the experimental conditions above and $A_{||}$ = 486.00 MHz, $g_{||}$ = 1.9460 for Species V.

The EPR features of VO^{2+} are able to reveal some details about how CD39 hydrolyzes ATP and ADP. A single EPR feature, species T, was observed when ADPNP (a non-hydrolyzable analog of ATP) complexed with VO^{2+} was bound to sCD39, which is consistent with the presence of only one nucleotide binding site [25]. The g and A tensors derived from species T are 1.9410 and 504.25 MHz respectively, which can be fitted best with one amino group and three groups combined from carboxyl and phosphate groups as the equatorial ligands of the bound VO^{2+} on sCD39. In accordance with metal-ATP complex coordination on other enzymes that hydrolyze ATP, like F_1-ATPase [22,28], the γ- and β-phosphate of ATP most likely bind to VO^{2+} while the third carboxyl group is contributed by a side-chain of aspartate or glutamate of sCD39. It is not unusual for the ε-amino group of lysine to coordinate with metals in enzymes. It has been reported that the amino group serves as one of VO^{2+} equatorial ligands in CF_1-ATPase [21], pyruvate kinase [19,20], AdoMet synthetase [17,18], and carboxypeptidase [16]. Thus one amino group from lysine, one carboxyl group from aspartate or glutamate, and two oxygens from the phosphates of ADPNP serve as the equatorial ligands of sCD39 bound VO^{2+} in the presence of ADPNP.

In the presence of AMPCP, bound VO^{2+} produced two EPR features, species D1 and species D2 that are separated by about 30 MHz. As we have reported that sCD39 releases intermediate ADP before ADP is further cleaved during ATP hydrolysis [25], sCD39 probably has two conformations that bind metal-ADP complexes, one is the conformation that releases the ADP intermediate, and another that recruits intermediate ADP back to the enzyme for further hydrolysis to AMP. However, intact CD39 does not release intermediate ADP during ATP hydrolysis, suggesting that there is only one ADP binding site on each CD39 monomer in the intact protein [2,25]. The two EPR species observed with VO^{2+}-AMPCP probably correspond to the two different conformations of bound ADP at the same catalytic site on sCD39. The signal intensity of the bound VO^{2+}-AMPCP EPR spectrum indicates that species D1 is dominant over species D2. In order to further assign species D1 and D2 to the two different conformations, two experiments were done (Fig. 5). Incubation of sCD39 with VO^{2+}-AMPCP at room temperature resulted in a dramatic decrease of the intensity of species D2, while the signal intensity of species D1 remained unchanged. These data indicate that VO^{2+}-AMPCP was released from the conformation corresponding to species D2; however, the conformation corresponding to species D1 still had bound VO^{2+}-AMPCP. More evidence for two conformations of the enzyme was obtained from the EPR spectra of bound VO^{2+}-ATP. No species T was found presumably because ATP was converted to ADP before the sample was frozen. Only species D2 was

observed and its intensity decreased as the incubation time was prolonged. We suggest that species D2 corresponds to the conformation that releases ADP as an intermediate product and species D1 corresponds to the conformation that binds ADP as a substrate. The lower signal intensities of species D1 and D2 compared to that of species T suggest that the affinity of sCD39 for ADP or its analog AMPCP is lower than that for the ATP analog ADPNP, which is consistent with the result that only ATP analogs were detected on sCD39 [25].

The calculated $g_{||}$ and $A_{||}$ values that best matched the experimental values for species D2 suggest that one hydroxyl group and three oxygens derived from carboxyl groups and phosphates are the equatorial ligands of bound VO^{2+}-ADP. Since the conformation corresponding to species D2 is found in the presence of ATP and is likely to be the conformation that releases bound VO^{+2}-ADP, it is likely that the VO^{+2} ligands are one phosphate and two carboxyl groups [25]. When ADP is the substrate and generates species D1, one water molecule and a combination of three groups between carboxyl groups and phosphates serve as the equatorial ligands of bound VO^{2+} on sCD39. The probable combination of carboxyl groups and phosphates for species D1 is one carboxyl group and two phosphates since VO^{2+} complexes ADP through two phosphates before VO^{2+}-ADP is bound to the enzyme.

The site directed mutagenesis studies on CD39 and other members of the CD39 family give some hints about the possible residues that serve as metal ligands at the catalytic site of sCD39. The changes of D62 on ACR1, E174 on ACR3, D213 (D219 in HB6) and S218 on ACR4 dramatically decrease both ATPase and ADPase activities of CD39 [12,15]. Figure 7 summarizes the possible coordination of Ca^{2+} from the data of species T, species D1, and species D2 in the different situations of sCD39 catalysis. The catalytic base attack results in cleavage of the γ-phosphate of ATP, and one carboxyl group replaces the γ-phosphate as a metal ligand (from species T to species D2), which is accompanied by a swap of an amino group with a hydroxyl group (S218?). This hydroxyl group (S218?) probably interacts with the water molecule through hydrogen bond in the conformation corresponding to species D1 to hydrolyze ADP. The constant carboxyl group that appears in all conformations of sCD39 hydrolysis is likely contributed by D213 since it is close to S218.

The results presented here also provide an explanation to the free metal inhibition of CD39 catalytic activity. Free VO^{2+} binds to sCD39 through two hydroxyl groups and two water molecules that are hydrogen bonded to other residues of sCD39. Once free VO^{2+} occupies the catalytic

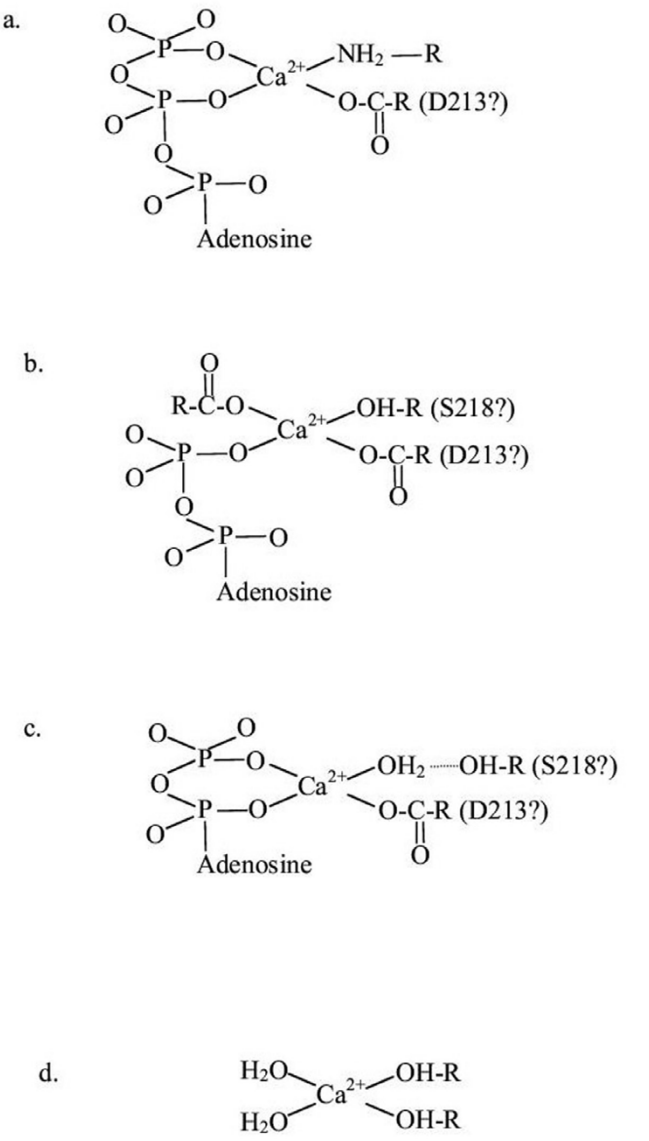

Figure 7
Summary of the ligands at the metal coordination sites of sCD39 during the catalytic reaction. The types of groups shown as equatorial ligands were derived from the best fits of ^{51}V hyperfine values from Table 2. a. The metal ligands in the presence of ADPNP (Species T) represent the conformation of ATP at the beginning of hydrolysis by sCD39. b. The metal coordination sites in the presence of AMPCP (Species D2) show the arrangement of the catalytic site prior to release of ADP as an intermediate product. c. The metal coordination sites in the presence of AMPCP (Species D1) show the conformation of the catalytic site ready to hydrolyze ADP. d. Metal coordination in the absence of nucleotide (Species V) showing the occupancy of the active site by free metal with exclusion of nucleotide and consequent inhibition of sCD39.

site, the enzyme has to either release the metal or correct the conformation before the substrates are recruited properly.

Conclusions

VO^{2+} can functionally substitute for Ca^{2+} as a cofactor for sCD39. Four different EPR spectra are obtained for VO^{2+} bound in the presence of different nucleotides and in the absence of nucleotide. The protein ligands for VO^{+2} in the presence of ATP are suggested to be carboxyl and amino groups, while those in the presence of ADP are probably carboxyl and hydroxyl groups. The mechanism of sCD catalysis is discussed. These results will provide guides for further studies of the catalytic mechanism of NTPDases.

Materials and Methods

Reagents

ATP, ADP, ADPNP, AMPCP were purchased from Sigma (St. Louis, MO). Zeocin, High-Five medium were purchased from Invitrogen (Carlsbad, CA).

Cell culture and preparation of soluble CD39

sCD39 transfected stable HighFive™ insect cells were cultured as described by Chen and Guidotti [25]. Soluble CD39 were purified as described [25] with some modifications. After concanavalin A-Sepharose 4B and nickel affinity column chromatography, the ammonium sulfate precipitated sCD39 was collected and resuspended in about 50 µl of 40 mM Tris-HCl (pH7.5). This sample was loaded on a Superose-12HR gel filtration column from Pharmacia Biotech equilibrated with 40 mM Tris-HCl (pH7.5). The fractions containing the major peak were collected, and the solvent was changed to 20 mM Hepes (pH8.0), 120 mM NaCl, 5 mM KCl with an YM30 centricon from Millipore. The final volume of the sample was around 200 µl, and the concentration of sCD39 was around 0.1 mM.

Concentrations of proteins were determined using D_C Protein Assay from BIO-RAD using the provided protocol.

Nucleotidase activity assay and nucleotide separation by HPLC

The reactions were carried out in 20 mM HEPES-Tris (pH 7.0), 120 mM NaCl, and 5 mM KCl; they were started by adding nucleotides at 37°C. After incubation for 15 minutes, the reactions were stopped with 2% perchloroacetic acid

Nucleotides were separated by HPLC on an anion exchange column (a 10 × 0.46 mm SAX column from Rainin Instruments) based on the method of Hartwick and Brown [29]. The low concentration buffer (A) was 0.08 M $NH_4H_2PO_4$ (pH3.8), and the high concentration buffer (B) was 0.25 M $NH_4H_2PO_4$ (pH4.95) with 8 mM KCl. The gradient used was 4 min, 0–2.5% (B); 26 min, 2.5–25% (B). Equilibration was done with buffer (A) for 10 minutes, and the flow rate was 1 ml/min.

Preparation of VO^{2+} solution

Vanadyl and nucleotide solution were prepared according to Houseman et al. [21]. Dissolved molecular oxygen was removed from solutions by purging with dry nitrogen gas. Stock vanadyl and nucleotide solution were thawed on ice, and mixed at 1:1 molar ratio by vigorous stirring. Then VO^{2+}-nucleotide complexes were added to purified sCD39 at 1:1 molar ratio, mixed, and incubated for 5 minutes on ice before they were transferred into EPR tubes. Once the samples were in EPR tubes, they were immediately frozen in liquid nitrogen, and stored in liquid nitrogen before using.

EPR Measurement

CW-EPR experiments were carried out at X-band (9 GHz) using a Bruker 300E spectrometer with a TE102 rectangular standard cavity and a liquid nitrogen flow cryostat operating at 150 K. Simulations of these EPR spectra were accomplished with the computer program QPOWA [30,31]).

To estimate the types of groups that serve as equatorial ligands to VO^{2+} in each condition, the observed values of $A_{||}$ derived from simulation of the EPR spectrum by QPOWA were compared with the coupling constants obtained from model studies [24,32] using:

$$A_{||calc} = \Sigma\, n_i A_{||i}/4$$

where i represents the different types of equatorial ligand donor groups, n_i (=1–4) is the number of ligands of type i, and $A_{||i}$ is the measured coupling constant for equatorial donor group i [24]. Similar equations were used to calculated $g_{||}$ from a given set of equatorial ligands for comparison with those derived experimentally.

Acknowledgement

This work was supported by Grant HL08893 from the National Institutes of Health.

References

1. Plesner L: **Ecto-ATPases: identities and functions.** *Int Rev Cytol* 1995, **158**:141-214
2. Zimmermann H, Braun N, Heine P, Kohring K, Marxen M, Sevigny J, Robson SC: **The molecular and functional properties of E-NTPDase1, E-NTPDase2 and Ecto-5' nucleotidase in nervous tissue.** *Proceedings of the Second International Workshop on Ecto-ATPase and Related Ectonucleotidases* 20009-20
3. Martin SS, Senior AE: **Membrane adenosine triphosphatase activities in rat pancreas.** *Biochim Biophys Acta* 1980, **602**:401-18
4. Hidalgo C, Gonzalez ME, Lagos R: **Characterization of the Ca2+- or Mg2+-ATPase of transverse tubule membranes isolated from rabbit skeletal muscle.** *J Biol Chem* 1983, **258**:13937-45

5. Obejero Paz CA, Gonzalez DA, Alonso GL: **Demonstration of the simultaneous activation of Ca2+-independent and Ca2+-dependent ATPases from rat skeletal muscle microsomes.** *Biochim Biophys Acta* 1988, **939**:409-15
6. Valente AP, Barrabin H, Jorge RV, Paes MC, Scofano HM: **Isolation and characterization of the Mg2(+)-ATPase from rabbit skeletal muscle sarcoplasmic reticulum membrane preparations.** *Biochim Biophys Acta* 1990, **1039**:297-304
7. Norton K, Moulton M, Rose R, Sabbadini R, Dahms AS: *Biophys. J* 1986, **49**:561a
8. Sabbadini RA, Dahms AS: **Biochemical properties of isolated transverse tubular membranes.** *J Bioenerg Biomembr* 1989, **21**:163-213
9. Handa M, Guidotti G: **Purification and cloning of a soluble ATP-diphosphohydrolase (apyrase) from potato tubers (Solanum tuberosum).** *Biochem Biophys Res Commun* 1996, **218**:916-23
10. Stout JG, Kirley TL: **Purification and characterization of the ecto-Mg-ATPase of chicken gizzard smooth muscle.** *J Biochem Biophys Methods* 1994, **29**:61-75
11. Schulte am Esch J 2nd, Sevigny J, Kaczmarek E, Siegel JB, Imai M, Koziak K, Beaudoin AR, Robson SC: **Structural elements and limited proteolysis of CD39 influence ATP diphosphohydrolase activity.** *Biochemistry* 1999, **38**:2248-58
12. Drosopoulos JHF, Broekman MJ, Islam N, Maliszewski CR, Gayle RB III, Marcus AJ: **Site-directed mutagenesis of human endothelial cell ecto-ADPase/soluble CD39: requirement of glutamate 174 and serine 218 for enzyme activity and inhibition of platelet recruitment.** *Biochemistry* 2000, **39**:6936-43
13. Grinthal A, Guidotti G: **Substitution of His59 converts CD39 apyrase into an ADPase in a quaternary structure dependent manne** *Biochemistry* 2000, **39**:9-16
14. Smith TM, Lewis Carl SA, Kirley TL: **Mutagenesis of two conserved tryptophan residues of the E-type ATPases: inactivation and conversion of an ecto-apyrase to an ecto-NTPase.** *Biochemistry* 1999, **38**:5849-57
15. Smith TM, Kirley TL: **Site-directed mutagenesis of a human brain ecto-apyrase: evidence that the E-type ATPases are related to the actin/heat shock 70/sugar kinase superfamily.** *Biochemistry* 1999, **38**:321-8
16. DeKoch RJ, West DJ, Cannon JC, Chasteen ND: **Kinetics and electron paramagnetic resonance spectra of vanadyl(IV) carboxypeptidase A.** *Biochemistry* 1974, **13**:4347-54
17. Markham GD: **Structure of the divalent metal ion activator binding site of S-adenosylmethionine synthetase studied by vanadyl(IV) electron paramagnetic resonance.** *Biochemistry* 1984, **23**:470-8
18. Zhang C, Markham GD, LoBrutto R: **Coordination of vanadyl(IV) cation in complexes of S-adenosylmethionine synthetase: multifrequency electron spin echo envelope modulation study.** *Biochemistry* 1993, **32**:9866-73
19. Tipton PA, McCracken J, Cornelius JB, Peisach J: **Electron spin echo envelope modulation studies of pyruvate kinase active-site complexes.** *Biochemistry* 1989, **28**:5720-8
20. Lord K, Reed GH: **Vanadyl(IV) complexes with pyruvate kinase: activation of the enzyme and electron paramagnetic resonance properties of ternary complexes with the protein.** *Arch Biochem Biophys* 1990, **281**:124-31
21. Houseman AL, Morgan L, LoBrutto R, Frasch WD: **Characterization of ligands of a high-affinity metal-binding site in the latent chloroplast F1-ATPase by EPR spectroscopy of bound VO2+.** *Biochemistry* 1994, **33**:4910-7
22. Chen W, LoBrutto R, Frasch WD: **EPR spectroscopy of VO2+-ATP bound to catalytic site 3 of chloroplast F1-ATPase from Chlamydomonas reveals changes in metal ligation resulting from mutations to the phosphate-binding loop threonine (betaT168).** *J Biol Chem* 1999, **274**:7089-94
23. Eaton SS, Eaton GR: **Vanadium in Biological Systems (Chasteen, N. D., Ed)** *Kluwer Academic Publishers, Dordrecht, The Netherlands* 1990199-222
24. Chasteen ND: **Biological Magnetic Resonance (Berliner, L., and Reuben, J., Eds)** *Plenum, New York* 199053-119
25. Chen W, Guidotti G: **Soluble apyrases release ADP during ATP hydrolysis.** *Biochem Biophys Res Commun* 2001, **282**:90-5
26. Weil JA, Hecht AG: **On the powder line shape of EPR spectra.** *J Chem Phys* 1963, **38**:281-286
27. Holyk N: **M. S. Thesis,** *University of New Hampshire, Durham, NH* 1979
28. Houseman AL, LoBrutto R, Frasch WD: **Effects of nucleotides on the protein ligands to metals at the M2 and M3 metal-binding sites of the spinach chloroplast F1-ATPase.** *Biochemistry* 1995, **34**:3277-85
29. Hartwick RA, Brown PR: **The use of high pressure liquid chromatography in clinical chemistry and biomedical research.** *Adv Clin Chem* 1980, **21**:25-99
30. Nilges MJ: **Electron Paramagnetic Resonance Studies of Low Symmetry Nickel (I) and Molybenum (V) Complexes, Ph.D. Thesis,** *University of Illinois, Urbana, IL* 1979
31. Maurice MJ: **Acquisition of Anisotropic Information by Computational Analysis of Isotropic EPR Spectra, Ph. D. Thesis,** *University of Illinois, Urbana, IL* 1980
32. Hamstra BJ, Houseman AL, Colpas GL, Kampf JW, LoBrutto R, Frasch WD, Pecoraro VL: **Structural and solution characterization of mononuclear vanadium (IV) complexes that help to elucidate the active site structure of the reduced vanadium haloperoxidases.** *Inorg Chem* 1997, **36**:4866-4874